CARBONATE SCAL: CHARACTERISATION OF CARBONATE ROCK TYPES FOR DETERMINATION OF SATURATION FUNCTIONS AND RESIDUAL OIL SATURATIONS

S.K. Masalmeh[*] and X.D.Jing
Shell International E&P, Rijswijk

This paper was prepared for presentation at the International Symposium of the Society of Core Analysts held in Abu Dhabi, UAE, 5-9 October, 2004

ABSTRACT
This paper presents a special core analysis (SCAL) study aimed at carbonate rock characterisation and measurement of saturation functions for modelling water-oil displacement of a heterogeneous reservoir. A particular focus is made on the measurement of water-oil capillary pressure curves using the centrifuge and CAPRICI - an in-house technique combining capillary pressure and resistivity measurements in multiple drainage and imbibition cycles. The basic rock characterisation includes thin section, SEM, NMR and mercury-air capillary pressure (Pc) measurements. Capillary pressure has been obtained in three cycles: oil displacing water starting from 100% water saturated plugs (primary drainage), water displacing oil starting from connate water after aging the plugs to restore reservoir wettability (imbibition) and finally oil displacing water starting from residual oil saturation (secondary drainage).

The data show that, for the particular carbonate reservoir under investigation, the fluid flow properties such as residual oil saturation and imbibition capillary pressure curves do not show consistent correlation with conventional rock typing or facies classification. For example, imbibition capillary pressure showed significant variations for a set of samples having similar permeability, porosity, and drainage capillary pressure curves. Insights into pore geometry and pore-scale physics are essential to explain the fluid displacement characteristics. Dynamic SCAL data (i.e., water displacing oil capillary pressure and relative permeability data) need to be included in the identification of rock types during reservoir characterisation.

The results of this study have important implications in the design, interpretation and application of laboratory SCAL programme and consequently on field development planning. Assigning saturation functions based on permeability or conventional rock typing is shown to be inadequate. Further research is needed to establish improved classification schemes for such types of heterogeneous carbonate reservoirs.

---

[*] Currently on assignment with Shell Abu Dhabi.

INTRODUCTION
Carbonate reservoirs are heterogeneous and often show mixed to oil-wet characteristics. Both heterogeneity and wettability have strong impact on relative permeability and imbibition capillary pressure curves and need to be taken into account when assigning the saturation functions in dynamic reservoir modelling. The complexity of carbonate reservoirs and the importance of a consistent approach in defining flow units or rock types have been a subject of several recent papers [1-7]. Current practices generally focus on static rock typing, which is either based on petrophysical properties (i.e., porosity, permeability and drainage Pc curves) or geological description (facies and depositional environment) or a combination of both. The underlying assumption is that static rock characterisation remains valid when assigning saturation functions in dynamic reservoir modelling. This approach of static rock typing and its applicability to describe dynamic data are investigated in this paper by incorporating conventional core analysis, mercury-air Pc, thin section and SEM analysis.

EXPERIMENTAL PROCEDURE
A detailed SCAL study was performed that aimed at the characterisation of carbonate rocks and the measurement of saturation functions for modelling water-oil displacement of a heterogeneous carbonate reservoir. More than 80 core samples have been drilled, cleaned and subjected to CT scanning. The permeability varies over four orders of magnitude ranging from less than a milliDarcy to more than a Darcy. The porosity of the field ranges mainly between 20 to 30% with also a few lower porosity units. In total 40 samples were selected for the subsequent SCAL experiments. The samples have been selected from different porosity and permeability ranges, however, in this paper we will focus on the 20 samples that have been selected from one porosity range (~ 27-30%).

A particular focus in this study is on the measurement of water-oil capillary pressure curves and residual oil saturations. The water-oil capillary pressure curves have been measured using a combination of centrifuge and CAPRICI [8]- an in-house technique combining capillary pressure and resistivity measurements in multiple drainage and imbibition cycles. While the centrifuge measures only the forced imbibition Pc curves, CAPRICI is able to measure the full Pc curves, i.e., both spontaneous and forced imbibition parts. Moreover, some samples have been used in separate spontaneous imbibition measurements which showed that there was hardly any spontaneous imbibition of water. Capillary pressure has been obtained in three cycles: oil displacing water starting from 100% water saturated plugs (primary drainage), water displacing oil starting from connate water after aging the plugs to restore reservoir wettability (imbibition) and finally oil displacing water starting from residual oil saturation (secondary drainage). In designing the centrifuge experiments the bond number [9] is always set to be below 10^{-5}.

The centrifuge experiments were performed using crude oil and synthetic brine at reservoir temperature. After primary drainage experiment the plugs were aged in crude

oil at 70 ^{o}C and 100 bars for four weeks. The CAPRICI experiments were performed at 100 ^{o}C. The capillary pressure (P_c), connate water (S_{wc}) and residual oil saturation (S_{or}) were obtained by numerical interpretation of the experimental data using MoReS (Shell in-house simulator). This numerical simulation approach is necessary for deriving the proper data as analytical interpretation does not take into account the full measurement physics (i.e., the non-uniform gravity in the plug during centrifuge experiment, capillary end effect, the interference of relative permeability with the build-up of the saturation profile in the sample) and therefore often give erroneous results [10].

EXPERIMENTAL RESULTS AND DISCUSSIONS

Figure 1 shows the plot of porosity vs. permeability of the sample set, indicating that the permeability varies by up to 4 orders of magnitude for almost the same porosity range. This is a typical trend for such kind of carbonate reservoirs which makes it very difficult to classify carbonate into rock types even for static reservoir modelling. This paper focuses on one porosity range (~ 27-30%), as described in Table 1.

Mercury/air (Hg-air) Capillary Pressure Measurements

Mercury/air capillary pressure curves and the derived pore-throat size distributions have been measured using small plugs of 15 mm in diameter and 22 mm long which have been drilled in the vicinity of the selected SCAL plugs. Since the mercury-air capillary pressure data is often used as a basis for rock typing especially when combined with porosity/permeability trends: a detailed study of the available Pc curves is performed to identify possible trends or correlations with different rock properties. These rock properties are permeability, rock classification, pore type etc. The Pc curves and pore throat size distribution data are shown in Figures 2-3.

Figure 2 shows Pc curves of all plugs in the porosity range of 27-30% while permeability ranges between 2 to 1000 mD. The following observations can be made:

1. There is a clear correlation between permeability and entry pressure [11]. The samples can be divided into three groups or permeability class where each group has almost one entry pressure:
    a. Group 1 of high permeability (40 - 1000 mD) shows very low entry pressure (0.1 to 1 psi oil/brine equivalent) and clear dual porosity system. The pore throat size distribution ranges between 1 to 1000 micrometer. Due to the dual porosity nature the Pc curves start with very low values initially, then increase steeply at wetting phase saturation of 50-70%. As saturation reaches 30% the Pc of these high permeability samples exceeds those of the lower permeability samples shown in the figure. This is also evident from the pore throat size distribution in Figure 3.
    b. Group 2 of medium permeability (10-25 mD) has an entry pressure of about 2 psi oil/brine equivalent and the capillary pressure increases as saturation decreases. There is a large transition zone and no clear plateau.

This indicates a wide range of pore size distribution but not a dual porosity system. As there are only three samples available in this study that belongs to this group, the above description cannot be generalised and more samples need to be included in future studies.

   c. Group 3 of low permeability (2-10 mD) has an entry pressure of 5-7 psi oil/brine equivalent and shows a clear plateau indicating a rather uniform pore size distribution.

2. The connate water of the three groups (at the same equivalent reservoir height above free water level) does not show a correlation with permeability. Some low permeable samples show lower connate water than some high permeable samples. This shows that any attempt to correlate connate water saturation with permeability, as often carried in sandstone reservoirs, is likely to fail here due to the complex pore systems.

Nuclear Magnetic Resonance (NMR) T2 Measurements

The NMR T2 measurements provide another means for characterising the pore (body) size distributions. NMR T2 relaxation spectrum measurements have been performed on all the plugs at 100% water saturation. For the plugs of permeability Group 1 (samples 1, 2, 5, 6, 7, 8) the spectra show dual porosity behaviours, see Figure 4. For the other samples (samples 10, 17 and 19) the plugs exhibit a uni-modal porosity system, similar to the pore throat size distribution obtained from the Hg-air measurement. Combining the results of the NMR and Hg-air measurements shows some important features such as the general average pore throat to pore body size ratios. For example, some samples show smaller pore throat sizes and yet larger pore body sizes. However the interpretation of NMR T2 distribution in carbonates and relating it to pore (body) size distribution is not quite straightforward. Some assumptions such as in the fast diffusion regime, and uniform surface relaxivity are often made in a general approach. Detailed pore network modelling of NMR response is recommended to take into account the full physics and relate NMR relaxation time distributions to corresponding pore (body) size distributions [12-13].

Thin Sections and SEM Analysis

All the samples used in this study (see Table 1) were prepared for thin section and SEM analysis. Each of the thin sections has a detailed petrographic description, concentrating on texture, composition, cements and diagenesis, and pore type. In addition, diagenetic evolution, depositional environment and reservoir properties were also briefly outlined. The samples have been classified using Dunham's textural classification for carbonate rocks [14]. The analysed samples predominantly consist of grainstones and packstones. Porosity habit and abundance in these samples is strongly affected by texture. Grainstone fabrics are generally characterised by good to very good and well to fairly well connected interparticle pores, followed by subordinate sparse to very sparse, usually isolated intraparticle porosity. Oversized pores, as well as micro-fractures are also locally present, with a certain amount of microporosity within granular components. Packstones are characterised by the progressive disappearance (with depth) of interparticle porosity

(ranging, in the uppermost samples, from good to sparse). The main porosity types of these lithologies consist of sparse to common mouldic porosity, coupled by sparse to rare intraparticle porosity.

No clear correlation was found between capillary pressure and the geological rock classifications. For example, grainstone samples in general have different capillary pressure, and some samples from different rock classes may have very similar drainage capillary pressure characteristics.

Primary Drainage Capillary Pressure
In addition to the mercury injection technique, primary drainage experiments have been performed using the centrifuge technique. The centrifuge data were interpreted using numerical simulation [10]. Similar to the mercury capillary pressure curves, the primary drainage capillary pressure curves measured on water-wet samples show a strong dependence on permeability. The connate (irreducible) water saturation of all plugs used in the centrifuge is 5% ±2%, independent of permeability as discussed in the Hg-air section above. There is no correlation between connate water and permeability or facies.

Qualitatively the centrifuge capillary pressure curves show the same trends compared to the Hg-air Pc curves. The question remains whether the Hg-air and water-oil Pc curves are identical for use in initialising the static reservoir models. It is a common practice to use Hg-air Pc curves to initialise static model and calculate oil in place. This is based on the assumption that Hg-air Pc curves can be converted to oil-water drainage Pc curves using the following equation:

$$Pc_R = Pc_L \frac{\sigma_R \cos(\theta)_R}{\sigma_L \cos(\theta)_L} \qquad\qquad (1)$$

where σ is the interfacial tension (IFT) between the two fluids, θ is the contact angle, subscript L refers to laboratory (Hg-air) and R refers to reservoir (oil-water). Figure 5 shows a comparison of Hg-air and centrifuge Pc curves. It shows a very good agreement between mercury-air and primary drainage centrifuge capillary pressure curves even for dual porosity rock. Hence, proper design and interpretation of centrifuge experiment can capture the impact of dual porosity on capillary pressure curves.

However, it is not always possible to find such close match between Hg-air and centrifuge oil/brine capillary pressure curves. This discrepancy is demonstrated in Figure 6 for samples from porosity range 20-24%. As shown in Figure 6, for this group of samples, the transition zone obtained from the Hg-air Pc is quite different than that obtained from the centrifuge Pc and initialising the static model using Hg-air Pc may give significant difference in initial oil in place and its distribution. This may also be one of the reasons why a mismatch is sometimes observed between log and Pc saturation height functions. Further investigation is needed in this topic area.

Leverett-J Function
Drainage capillary pressure is used to initialise reservoir static model, i.e., to determine saturation as a function of height above free water level (FWL) and to calculate stock tank oil initially in place (STOIIP) or gas initially in place (GIIP) of hydrocarbon reservoirs. Since usually a limited number of capillary pressure curves are available, different models have been developed to relate capillary pressure curves with porosity and permeability, and to generate saturation vs. height functions [15]. The Leverett J-function is one of the most commonly used formulations:

$$J(S_w) = \frac{P_c}{\sigma \cos(\theta)} \sqrt{\frac{K}{\varphi}} \qquad (2)$$

The J-function was originally proposed to convert all capillary pressure data for clean sands to a universal curve. However, this formulation has also been used for shaly sands and for carbonates. Carbonate reservoirs are known for their complex pore geometry which may cause the J-function approach to break down. The data measured on the reservoir core under study is used to check the applicability of the J-function. Figure 7a shows the drainage Pc curves for plugs of permeability Group 1 ($40 < K < 1000$ mD). As discussed above the Pc curves can be presented by almost one curve, there is hardly any dependence on permeability within this permeability range. Converting the Pc curves into a J-function (see figure 7b) generates three distinct groups with quite different J-functions. This shows that for heterogeneous dual porosity rock the use of a general J-function is prone to errors, and the J-function should only be used with sufficient core data support and careful sub-zonation when initialising the static model.

Initialising the Static Model
The above discussion shows that using an average J-function to calculate Pc curves and saturation height functions may lead to serious errors in calculating hydrocarbon in place especially for dual porosity system. For the reservoir under study and for the porosity range 27-30%, the data suggests that for each permeability range one average Pc curve can be used to initialise the static model, without the need to apply J-function or permeability scaling. Note that the low permeable samples (2-10 mD) may still be divided into two groups for a more accurate initialisation.

Imbibition and Secondary Drainage Pc Curves
The imbibition and secondary drainage Pc curves have been measured for a number of plugs, see Figures 8 and 9. The measured experimental data were interpreted using numerical simulation. The data show a general trend of increasing the negative capillary entry pressure ($P_c = P_o - P_w$) as the permeability decreases, see Figure 8. Figure 9 shows that the secondary Pc curves of almost all plugs are the same, there is no correlation with permeability, primary drainage capillary pressure or facies.

Both imbibition and secondary drainage Pc curves show different behaviour as compared to primary drainage Pc curves. The main observations are summarised below:

1. No correlation between permeability and residual oil saturation (Sor). The residual oil saturation varies between 5 to 18% for plugs of the same permeability, and the same Sor is found for several samples of different permeability values.
2. Figure 8 shows that the samples can be divided into two groups.
    a. High permeable samples (s1-s9) show no noticeable entry pressure but the imbibition Pc decreases (becomes more negative) as the water saturation increases, and close to residual oil saturation the Pc curves of some high permeable samples become lower (more negative) than that of the low permeable samples.
    b. Low permeable samples (s10-20) have a clear entry pressure that varies between –2.5 to –4.5 psi oil/brine, and then a plateau extends until almost residual oil saturation.
3. The simple static rock typing presented above cannot be used to assign imbibition and secondary drainage Pc curves in the dynamic reservoir modelling.
4. The shape of the imbibition and secondary drainage Pc curves cannot be inferred from that of the primary drainage Pc curves, i.e., for example dual porosity is evident for high permeable samples from primary drainage Pc data while it cannot be seen in the imbibition and secondary drainage Pc data.
5. Secondary drainage Pc curves are almost identical, with some differences only found close to the connate water.
6. The connate water saturation after secondary drainage is in general higher than that after primary drainage as previously reported [11].

The above shows that static rock typing based on porosity, permeability and drainage capillary pressure does not provide an adequate basis for consistently assigning dynamic saturation functions. Different rock type classification is needed for dynamic modelling, i.e., dynamic data (e.g., imbibition Pc, relative permeability and residual oil saturations) need to be used for dynamic rock typing. Note that the difference in the dynamic data is not due to the wettability variation against reservoir depth, as reported in [7]. All the samples in this study have been subjected to the same cleaning, restoration and drainage Pc procedures.

The question remains how to explain the different behaviour of the samples, especially those that had similar static properties but different imbibition Pc and Sor. Close inspection of the data shown in Figure 10, reveals that there is almost a factor 2 difference in the imbibition entry pressure while the difference in the drainage entry pressure is minimal. The four samples have the same connate water while they have different residual oil saturation. In particular samples s17 and s18 have the same drainage and imbibition entry pressure but they have different Sor of 18% and 5%, respectively. The large difference in Sor can be qualitatively explained by using the SEM data of those two samples, see Figure 11. The SEM pictures show that sample s17 has some macropores surrounded by, and connected to a porous system dominated by micro pores, which can result in higher trapping of oil in the large pores or vugs. On the other hand, sample 18 is predominantly a microporosity system that has very good connectivity.

Proper modelling of fluid flow in this kind of complex carbonate needs detailed description of the pore network geometry and topology as well as correct representation of pore-scale physics.

In summary, while the four samples shown in Figure 10 can be considered one rock type if classified based on static data (i.e., porosity, permeability and primary drainage capillary pressure), dynamic data (e.g., imbibition capillary pressure and residual oil saturation) show that they at least should be divided into three different groups or dynamic rock types. For heterogeneous carbonate reservoirs this difference in imbibition capillary pressure can have significant impact on waterflood recovery [16]. Different Sor will also mean different relative permeability curves for these samples. Based on the measured SCAL data an appropriate capillary pressure model, in addition to the relative permeability model, is needed to capture the wide range of Pc shapes both in drainage and in imbibition. Moreover, a new dynamic rock typing approach is also needed to assign relevant capillary pressure and relative permeability curves to each flow cell, taking into account static and dynamic data.

CONCLUSIONS

A detailed special core analysis study has been carried out on rock samples selected from a heterogeneous carbonate reservoir. A bi-modal pore size distribution is evident based on the mercury injection capillary pressure curves, especially for the high permeable plugs. The following conclusions can be drawn from this study:

1. The primary drainage entry pressure increases as the permeability decreases but the capillary pressure, permeability and porosity relationship does not follow any clear Leverett-J trends. The data show that the applicability of the classic Leverett-J function for the carbonate reservoir under investigation needs to be carefully checked against SCAL data due to the heterogeneity and complex pore structure.

2. There is no general correlation between static rock typing and dynamic properties. The imbibition capillary pressure data show that low permeable samples have higher negative entry pressure than high permeable samples. However, correlating imbibition Pc with permeability alone may be misleading. Pore scale geometry and wettability physics need to be incorporated for proper classification of imbibition Pc curves including both the entry pressure, shape and end-point residual oil saturation. In addition, the secondary drainage Pc curves show hardly any permeability dependence.

3. Static rock typing (based on porosity, permeability, primary drainage capillary pressure or geological facies description) has been found to be inadequate for such kind of heterogeneous carbonates with bi-modal pore size distributions and complex mixed wettability characteristics. New dynamic rock typing schemes are needed to take into account dynamic displacement data such as imbibition capillary pressure, relative permeability and residual oil saturation for proper modelling of waterflooding and any possible subsequent IOR processes.

REFERENCES

1- Marzouk, I., Takezaki, H and Suzuki, M.: "New Classification of Carbonate Rocks for Reservoir Characterization", SPE 49475, 9th ADIPEC, Abu Dhabi, Oct. 15-18, 2000.

2- Ramakrishnan, T.S., Rabaute, A. Fordham, E.J., Ramamoorthy, R., Herron, M., Matteson, A. and Raghuraman, B.: "A petrophysical and Petrographic Study of Carboante Cores from the Thamama Formation", SPE 49502, 9th ADIPEC, Abu Dhabi, Oct. 15-18, 2000.

3- Leal, L., Barbato, R., Quaglia, A., Porrai, J.C. and Lazarde, H.: "Bimodal Behavior of Mercuri-Injection Capillary Pressure Curve and Its Relationship to Pore Geometry, Rock-Quality and Production Performance in Laminated and Heterogeneous Reservoirs", SPE 69457, SPE Latin America and Caribbean Petroleum Engineering Conference, Buenos Aires, March 25-28, 2001.

4- Porrai, J.C. and Campos, O.: "Rock Typing: A key Approach for Petrophysical Characterization and Definition of Flow Units, Santa Barbara Field, Eastern Venezuela Basin", SPE 69458, SPE Latin America and Caribbean Petroleum Engineering Conference, Buenos Aires, March 25-28, 2001.

5- Giot D., Dawans J.M., King, R. and Lehmann, P.: "Tracking Permeability in Major Limestone Reservoir: From Rock Observation to 3D Modelling", SPE 87233, 9th ADIPEC, Abu Dhabi, Oct. 15-18, 2000.

6- Silva, F.P.T., Ghani, A., Al Mansouri, A. and Bahar, A.: "Rock Type Constrained 3D Reservoir Characterization and Modelling", SPE 78504, 10th ADIPEC, Abu Dhabi, Oct. 13-16, 2002.

7- Hamon, G.: "Two –Phase Flow Rock-Typing: Another Perspective", SPE 84035, SPE Annual Technical Conference and Exhibition, Denver, Colorado, Oct. 5-8, 2003.

8- Kokkedee, J.A., Boutkan, V.K.: "Towards Measurement of Capillary Pressure and Relative Permeability at Representative Wettability", European Symposium on Improved Oil Recovery, Moscow, 1993.

9- O'Meara Jr., D.J., Hirasaki, G.J. and Rohan, J.A.: "Centrifuge Measurements of Capillary Pressure: Part 1- Outflow Boundary Conditions", SPE 18296, SPE Annual Technical Conference and Exhibition, Houston, Texas, Oct. 2–5, 1988.

10- Maas, J.G. and Schulte, A.M.: "Computer Simulation of Special Core Analysis (SCAL) flow Experiments Shared on the Internet", SCA-9719, Calgary, Canada, Sept. 7-10, 1997.

11- Masalmeh, S.K.: "The Effect of Wettability on Saturation Functions and Impact on Carbonate Reservoirs in the Middle East ", SPE 78515, 10th ADIPEC, Abu Dhabi, Oct. 13-16, 2002.

12- Moctezuma, A., Békri, S. Laroche, C. and Vizika O. "A Dual Network Model for Relative Permeability of bimodal rocks: Application in a Vuggy Carbonate", SCA 2003-12, Pau, France, Sept. 22-25, 2003.

13- Valvatne, P.H., Jing X.D. and Smits, R.M.M. "Modelling Pore Geometric and Wettability Trends of Multiphase Flow in Porous Media", SCA 2004 (this volume), Abu Dhabi, UAE, Oct. 5-9, 2004

14- Dunham, R.J., 1962. Classification of carbonate rocks according to depositional textures. In: Ham, W.E. (ed.) Classification of carbonate rocks. Memoir American Association of Petroleum Geologists, 1, 108-121.

15- Harrison, R. and Jing, X.D. "Saturation Height Methods and Their Impact on Volumetric Hydrocarbon in Place Estimates", SPE 71326, SPE Annual Technical Conference and Exhibition, New Orleans, Louisiana, Sept. 30– Oct. 3, 2001.

16- Masalmeh, S.K., Jing, X.D., van Vark, V., Christiansen, S., van der Weerd, H. and van Dorp, J. "Impact of SCAL on Carbonate Reservoirs: How Capillary Forces Can Affect Field Performance Predictions", SCA 2003-36, Pau, France, Sept. 22-25, 2003.

Table 1: Characteristics of samples used in the study

| Sample	Depth	Rock Classification	Porosity	K_air	K_brine	Grain density
no.	[ft]	(Dunham, 1962)	[%V_b]	[mD]	[mD]	[g/cm^3]
s1	8593.40	Peloidal grainstone	31.6	400	348	2.708
s2	8593.80	Peloidal grainstone	30.5	50	37	2.706
s3	8595.30	Pack-grainstone	29.2	28	25.3	2.704
s4	8619.50	Pack-grainstone	27.3	14	13.5	2.705
s5	8620.20	Peloidal grainstone	30.8	260	197	2.708
s6	8622.20	Peloidal grainstone	30.2	73	53	2.709
s7	8622.90	Peloidal grainstone	31.1	103	78	2.707
s8	8626.90	Intraclastic-peloidal grainstone	29.8	1010	833	2.709
s9	8636.65	Packstone	30.4	14	10.4	2.706
s10	8658.30	Dolomitic peloidal grainstone/packstone	28.0	7.3	4.7	2.727
s11	8659.35	Packstone	28.1	6.9	5.6	2.723
s12	8660.93	Pack-wackestone	29.7	8.2	7.6	2.718
s13	8661.43	Packstone	28.3	5.5	3.5	2.712
s14	8661.70	Wacke-packstone	29.0	6.6	4.2	2.713
s15	8662.20	Peloidal grainstone	28.7	8.6	4.9	2.714
s16	8670.50	Packstone	28.0	4.7	3.6	2.716
s17	8702.20	Peloidal packstone	29.1	5.5	3.4	2.724
s18	8709.80	Peloidal packstone	30.2	4.6	2.6	2.723
s19	8711.60	Peloidal packstone	27.9	4.1	2.3	2.722
s20	8719.40	Peloidal packstone	28.8	4.5	2.5	2.717
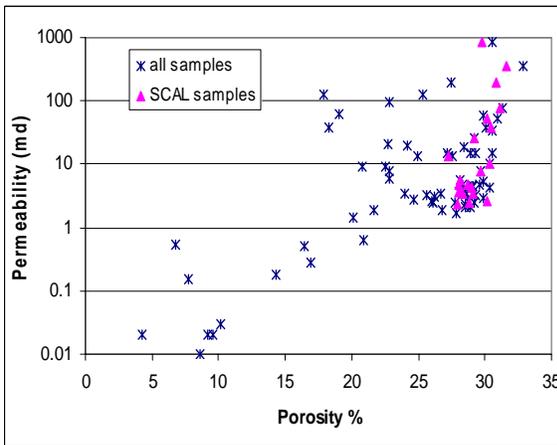
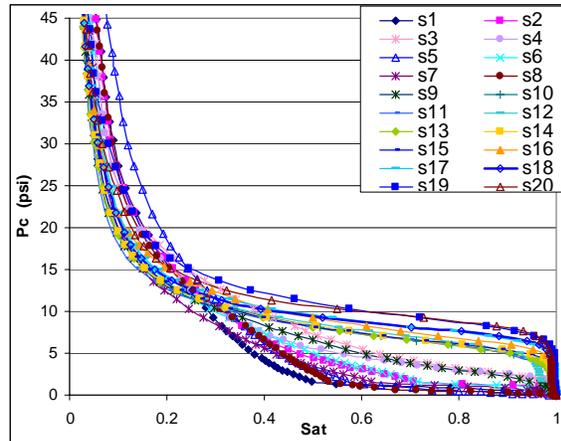Figure 1: Porosity vs Permeability of the sample set

Figure 2: Hg - air capillary pressure curves for the sample set (converted to oil – brine system)
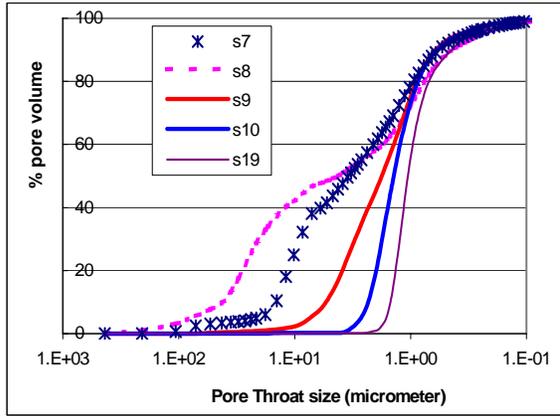
Figure 3: Pore throat size distribution of selected samples.
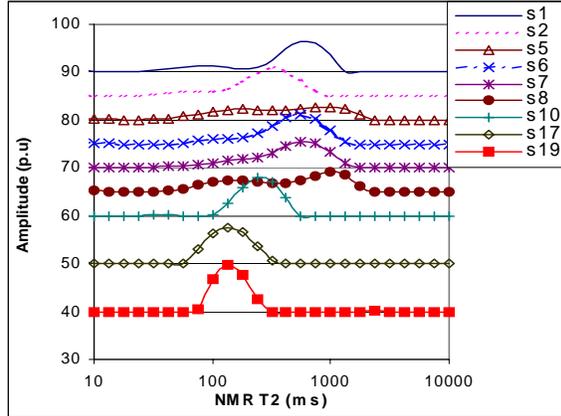

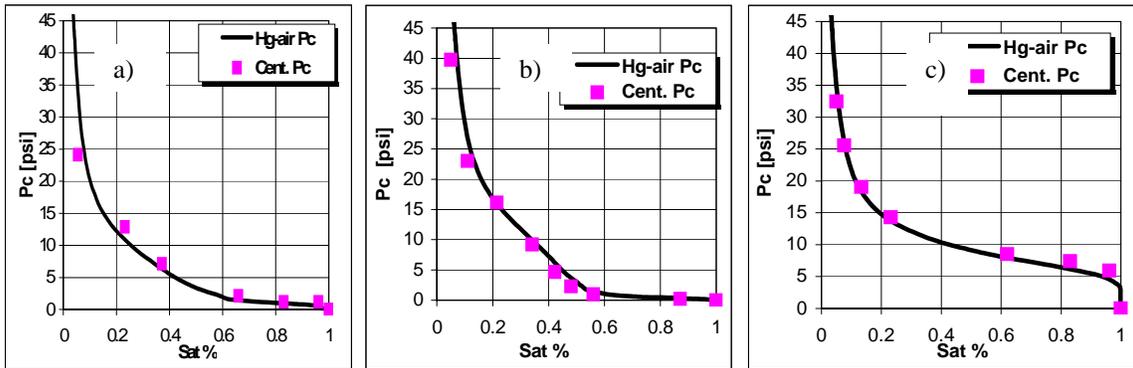
Figure 4: NMR T2 distribution of selected samples.

Figure 5: Comparing Centrifuge to Hg-air Pc curves for porosity range 27-32%, a) s7, b) s8 and c) s10.
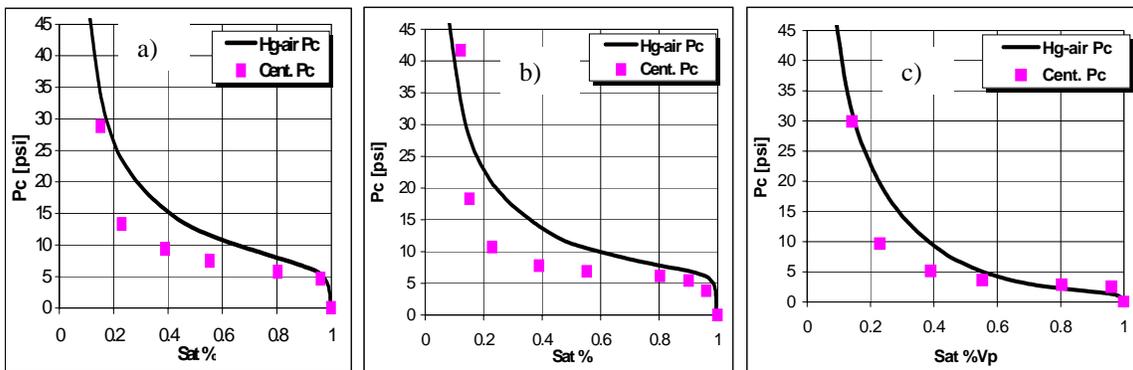

Figure 6: Comparing Centrifuge to Hg-air Pc curves for porosity range 20-24% and the permeability of the samples are: a) K=1.4 md, b) K=1.9 md and c) K=13.6 md.

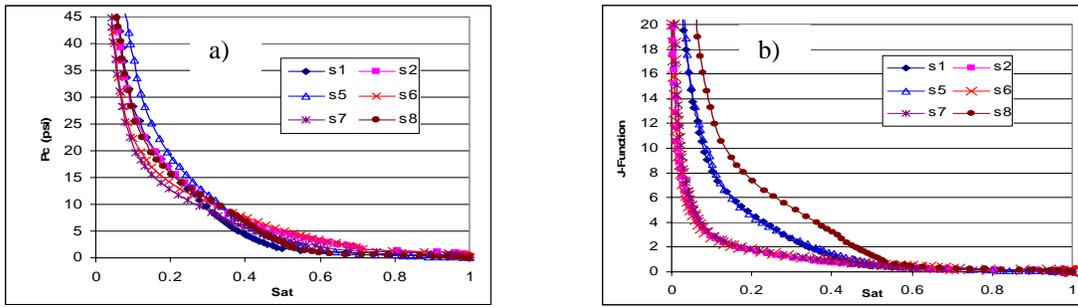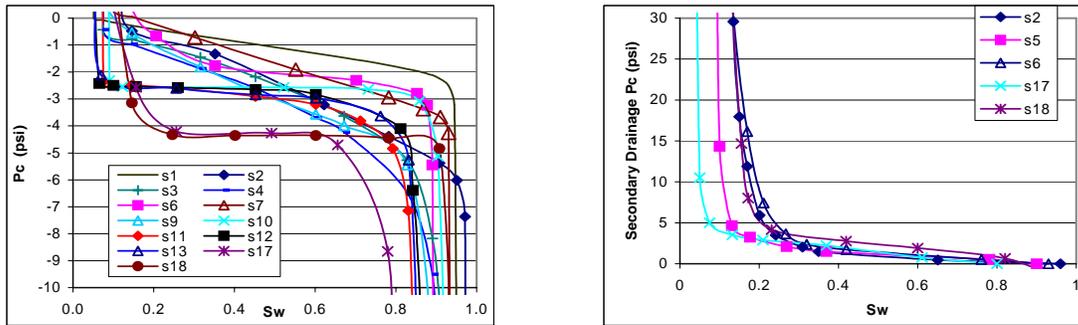Figure 7: a) Pc curves for high permeability samples, b) Leverett J-Function for the same samples.

Figure 8: Imbibition Pc curves.

Figure 9: Secondary drainage Pc curves.
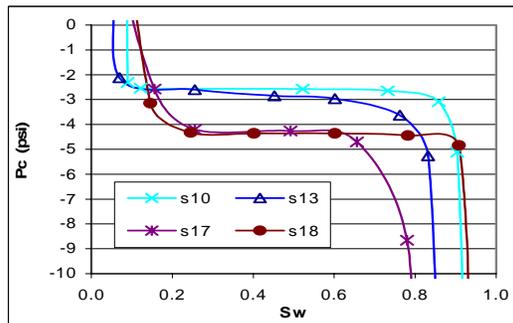

Figure 10: Imbibition Pc curves of selected 4 samples that show variation in entry pressure and/or Sor while drainage Pc, porosity and permeability are very similar.

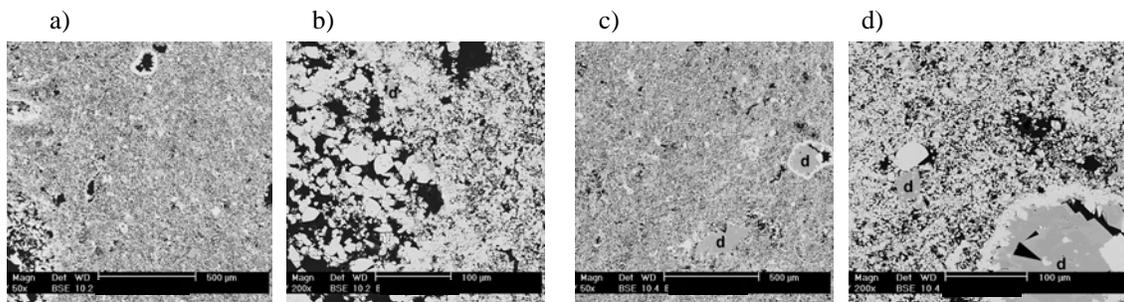a)   b)   c)   d)

Figure 11: SEM pictures of samples s17 (a&b) and s18 (c&d). The figures show that sample s17 has some isolated large pores (vugs) which leads to more oil trapping during imbibition. It qualitatively explains the high Sor value for sample s17 compared to sample s18.